ORIGINAL ARTICLE

Cancer Science WILEY

Biallelic loss of *FAM46C* triggers tumor growth with concomitant activation of Akt signaling in multiple myeloma cells

Jo Kanasugi[1] | Ichiro Hanamura[1] [iD] | Akinobu Ota[2] [iD] | Sivasundaram Karnan[2] [iD] | Vu Quang Lam[1] | Shohei Mizuno[1] | Md Wahiduzzaman[2] | Md Lutfur Rahman[2] | Toshinori Hyodo[2] | Hiroyuki Konishi[2] | Shinobu Tsuzuki[2] | Yoshitaka Hosokawa[2] | Akiyoshi Takami[1]

[1]Division of Hematology, Department of Internal Medicine, Aichi Medical University, Nagakute, Japan

[2]Department of Biochemistry, Aichi Medical University, Nagakute, Japan

Correspondence
Akinobu Ota, Department of Biochemistry, Aichi Medical University School of Medicine 1-1 Yazakokarimata, Nagakute, Aichi 480-1195, Japan.
Email: aota@aichi-med-u.ac.jp

Ichiro Hanamura, Division of Hematology, Department of Internal Medicine, Aichi Medical University School of Medicine, 1-1 Yazakokarimata, Nagakute, Aichi 480-1195, Japan.
Email: hanamura@aichi-med-u.ac.jp

Abstract

Loss of heterozygosity or mutation of the family with sequence similarity 46, member C (*FAM46C*) gene on chromosome band 1p12 is associated with shorter overall survival of patients with multiple myeloma (MM). In this study, using human MM cell lines (KMS-11, OCI-My5, and ANBL-6), we generated *FAM46C*$^{-/-}$ cell clones and examined the effect of disruption of *FAM46C* on cell survival and cellular signaling. Cell proliferation assays showed increased clonogenicity of *FAM46C*$^{-/-}$ KMS-11 cells compared to WT cells. Xenograft experiments showed significantly shorter overall survival of mice harboring the *FAM46C*$^{-/-}$ cell-derived tumors than mice with the *FAM46C*^{WT} cell-derived tumors. Notably, levels of phosphorylated Akt and its substrates increased both in vitro and in vivo in the *FAM46C*$^{-/-}$ cells compared to WT cells. In addition, caspase activities decreased in the *FAM46C*$^{-/-}$ cells. Results of gene set enrichment analysis showed that loss of *FAM46C* significantly activated serum-responsive genes while inactivating phosphatase and tensin homolog (PTEN)-related genes. Mechanistically, loss of FAM46C decreased the PTEN activity, number of apoptotic cells, and caspase activities. PF-04691502, a selective PI3K inhibitor, suppressed the augmented phosphorylation of Akt and its substrate FoxO3a. Treatment with afuresertib (a specific Akt inhibitor) in combination with bortezomib additively decreased *FAM46C*$^{-/-}$ MM cell survival. Collectively, this study is the first to report that loss of *FAM46C* triggers the concomitant activation of the PI3K-Akt signaling pathway, which might be a therapeutic target for MM with abnormalities in the *FAM46C* gene.

KEYWORDS

FAM46C, multiple myeloma, PI3K-Akt, tumor suppressor, tumorigenesis

---

Kanasugi, Hanamura, and Ota contributed equally to this work.

1 | INTRODUCTION

Multiple myeloma (MM) is a complex plasma cell neoplasm, accounting for approximately 10% of all hematological malignancies.[1-3] Novel genetic evidence showed highly heterogenous molecular characteristics in patients with MM even within similar tumor types, and association of specific genetic abnormalities with the clinical outcome in patients with MM.[4-10] One of the chromosomal aberrations, deletion of 1p12, was associated with shorter overall survival (OS) of patients with MM.[11] In recent decades, whole-genome sequencing approaches enabled the genomic analysis of myeloma. Somatic mutations and deletion in the *FAM46C* gene, located at 1p12, were detected in both patient-derived MM cells and cell lines.[12,13] Because *FAM46C* has the fourth-highest mutation frequency in MM,[12,14] it is important to understand the molecular basis underlying the involvement of mutation or deletion of *FAM46C* in the pathophysiology of MM.

FAM46C, also designated as terminal nucleotidyltransferase 5C (*TENT5C*), is located on chromosome 1p12. Loss of heterozygosity or mutation of the *FAM46C* gene has been identified in 5% to 13% of the patients.[7-9,12,14] The *FAM46C* gene abnormality has emerged as a novel predictor for shorter overall survival of patients with myeloma.[15] Recently, Zhu et al[16] reported that loss of *FAM46C* promotes cell survival in MM cells. In addition, Mroczek et al[17] reported that *FAM46C* acts as a tumor suppressor in MM through the activity of non-canonical poly(A) polymerase. Although these studies elucidated the tumor-suppressive role of FAM46C in MM cells, the relationship between loss of FAM46C and cellular signaling related to MM cell survival is still obscure.

In this study, we generated *FAM46C*-deficient human MM cells using clustered regularly interspaced short palindromic repeats (CRISPR)-Cas9 technology and investigated whether disruption of FAM46C affects cell growth, both in vitro and in vivo. We also describe the molecular mechanisms by which loss of FAM46C confers proliferative and survival advantage to MM cells.

2 | MATERIALS AND METHODS

2.1 | Reagents

RPMI-1640, penicillin-streptomycin solution, and trypsin-EDTA solution were purchased from Wako Pure Chemical Industries. Plasmid pMSCV-flag-myr-Akt1-IRES-GFP was a gift from Kira Gritsman and Jean Zhao (plasmid #65063; Addgene).[18] Plasmid pMSCV-IRES-GFP II (pMIG II) was a gift from Dario Vignali (plasmid #52107; Addgene).[19] Thiazolyl blue tetrazolium bromide (MTT) was purchased from Sigma-Aldrich Japan. Rabbit polyclonal anti-FAM46C Ab was obtained from Proteintech. Lenalidomide (LEN), pomalidomide (POM), bortezomib (BOR), PI3K inhibitor (PF-0469162), 3-phosphoinositide dependent protein kinase 1 (PDPK1) inhibitor (OSU-03012), and Akt inhibitor (afuresertib) were from Selleck Chemicals.

2.2 | Cell culture

Human MM cell lines KMS-11, RPMI8226, KMM1, and FLAM-76 were obtained from the Japanese Collection of Research Bioresources Cell Bank. The human MM cell line, UTMC-2, was kindly provided by Dr Shuji Ozaki (Tokushima Prefectural Central Hospital).[20] Interleukin (IL)-6-dependent MM cell line ANBL-6 was kindly provided by Dr Diane F. Jelinek (Mayo Clinic).[21] KMS-11 and OCI-My5 cells were maintained in RPMI-1640 supplemented with 10% FBS (Nichirei Biosciences). The IL-6-dependent ANBL-6 cells were maintained in RPMI-1640 medium supplemented with 10% FBS in the presence of recombinant human IL-6 (10 ng/mL; R&D Systems) at 37°C in a 5% CO_2 humidified atmosphere.

2.3 | Reverse transcription-PCR and sequence analysis

The RT-PCR analyses were undertaken as previously described.[22] The ORF of *FAM46C* was amplified using KOD Fxneo polymerase (Toyobo) and a specific primer set as described in Table S1. Sanger sequencing analysis was carried out using the BigDye Terminator version 3.1 Cycle Sequencing Kit (Thermo Fisher Scientific) and ABI 3500 Genetic Analyzer (Thermo Fisher Scientific).

2.4 | *FAM46C* gene knockout using CRISPR-Cas9 system

The CRISPR-Cas9 system was used to disrupt the expression of the *FAM46C* gene, as described previously.[23] pSpCas9(BB)-2A-GFP (PX458) and lentiCRISPR v2 were gifted by Feng Zhang (plasmid #48138 for PX458 and plasmid #52961 for lentiCRISPR v2; Addgene).[24,25] A single guide RNA (sgRNA) sequence was selected using E-CRISP (http://www.e-crisp.org/E-CRISP/designcrispr.html). The sgRNA sequences for *FAM46C* exon-2 are shown in Table S1. For lentivirus preparation, 293T cells (4×10^6 cells/dish) were seeded in a 10-cm dish 1 day before transfection. Lentiviral lentiCRISPR v2 containing *FAM46C* sgRNA, viral packaging vector psPAX2 (a gift from Didier Trono; plasmid #12260; Addgene), and viral envelope vector pCMV-VSV-G (a gift from Bob Weinberg; plasmid #8454; Addgene)[26] were diluted at 4:3:2 ratio in Opti-MEM medium (Thermo Fisher Scientific). A single clone was selected from a 96-well plate, expanded in a 12-well plate, and used for biological assays.

2.5 | Cell viability (MTT) assay

The MM cells were seeded in 96-well culture plates (1×10^4 cells/well) and incubated in the culture medium. After incubation for 72 hours, an MTT assay was carried out as described previously.[23] The absorbance at 545 nm was measured using a SpectraMAX M5 spectrophotometer (Molecular Devices).

2.6 | Annexin V assay

The MM cells were seeded in 6-well culture plates (5×10^5 cells/well) and incubated in the culture medium for 48 hours, followed by incubation with annexin V (AxV)-FITC (Medical & Biological Laboratories) at room temperature (25°C) for 15 minutes. Finally, fluorescence intensities were determined by FACS using FACSCantoII (BD Biosciences).

2.7 | Cell cycle analysis

The MM cells (5×10^5 cells/well) were seeded and incubated as described above. Cell cycle analysis was undertaken as described previously.[27] Briefly, the cultured cells were fixed in ice-cold 70% ethanol overnight. After fixation, the cells were treated with RNase A (100 µg/mL) and stained with propidium iodide (PI; 100 µg/mL). The cell cycle was analyzed with FACSCanto II (BD Biosciences). The percentages of cells in the sub-G_1, G_1, S, and G_2-M phases were measured using FlowJo software (Tree Star).

2.8 | Cellular caspase-3/7 activity assay

The caspase-3/7 assay was undertaken using a Caspase-Glo 3/7 Assay Systems (Promega) following the manufacturer's instructions. Briefly, cells (1×10^4 cells/well) were seeded in a 96-well culture plate and incubated for 24 hours. After the incubation, the cell suspension was transferred to a 96-well white plate (Thermo Fisher Scientific) and 100 µL of caspase-3/7 reagent was added to each well. Luminescence was measured using a SpectraMax M5 spectrophotometer (Molecular Devices). For normalization, data were expressed relative to caspase-3/7 activity in parental cells, which was arbitrarily set at 100%.

2.9 | Western blot analysis

Western blot analysis was carried out as described previously.[28] The Abs used in this study are described in Table S2. Immune complexes were detected using ImmunoStar LD (Wako Pure Chemical Industries) in conjunction with Amersham Imager 600 (GE Healthcare).

2.10 | Gene expression analysis

FAM46C-WT and *FAM46C*-KO MM cell clones were seeded in a 6-well plate (5×10^5 cells/well) and incubated for 48 hours. Total RNA was extracted using NucleoSpin RNA with DNase treatment (TaKaRa Bio). The experimental procedure for the cDNA microarray analysis was based on the manufacturer's protocol (Agilent Technologies), and as described previously.[23] The Cy3-labeled cRNA was purified, fragmented, and hybridized onto a SurePrint G3 Human Gene Expression 8 × 60K v3 Chip containing 26 083 Entrez Gene RNAs, using a Gene Expression Hybridization kit (Agilent Technologies). The raw and normalized microarray data have been submitted to the GEO database at NCBI (GSE119451; https://www.ncbi.nlm.nih.gov/geo/query/acc.cgi?acc=GSE119451). Gene set enrichment analysis (GSEA) was undertaken according to the instructions (https://software.broadinstitute.org/gsea/index.jsp).[29,30]

2.11 | Soft-agar colony formation assay

FAM46C-WT and *FAM46C*-KO KMS-11 cell clones (1×10^3 cells/well) were cast in 2 mL of 0.4% agarose (top-layer) (Bacto agar; BD Biosciences) and poured on top of a 2 mL of 0.6% agarose (bottom layer) in 6-well plates. After incubation for 14-17 days, the colonies were stained with MTT solution (5 mg/mL) in PBS. Photographs were taken under bright-field microscopy using a microscope (IX-73; Olympus).

2.12 | Xenograft experiment

Female FOX CHASE SCID C.B-17/lcr-scid/scidJcl mice were purchased from CLEA Japan. Mice were bred at the Institute of Animal Experiments, Aichi Medical University and 6- to 8-week-old mice were used in the experiments. The *FAM46C*-WT or *FAM46C*-KO KMS-11 and OCI-My5 cell clones (2×10^7 cells) were injected into the s.c. space in the backside of Scid mice. Tumors were measured every 3 or 4 days, and tumor volumes were calculated using the modified ellipsoid formula $1/2(\text{length} \times \text{width}^2)$. Mouse survival was analyzed with Kaplan-Meier-based method (n = 6).

2.13 | Statistical analysis

Results are expressed as mean ± SE. Statistical significance between groups was determined using one-way ANOVA and Student's *t* test. Statistical analyses were carried out using the SPSS 23.0 program (SPSS) and EZR software.[31]

3 | RESULTS

3.1 | Disruption of FAM46C promotes tumorigenicity of myeloma cells

We first undertook western blot analysis to investigate FAM46C protein expression level using a series of human MM cell lines. Among the 12 human MM cell lines, FAM46C protein expression was detectable in KMS-11, OCI-My5, U266, ANBL-6, RPMI8226, AMU-MM1, INA-6, and FLAM-76 cells. However, it was barely detectable in the UTMC-2 and NCU-MM1 cells (Figure 1A). The FISH analysis with FAM46C/134N8 probe showed the loss of 1 copy of
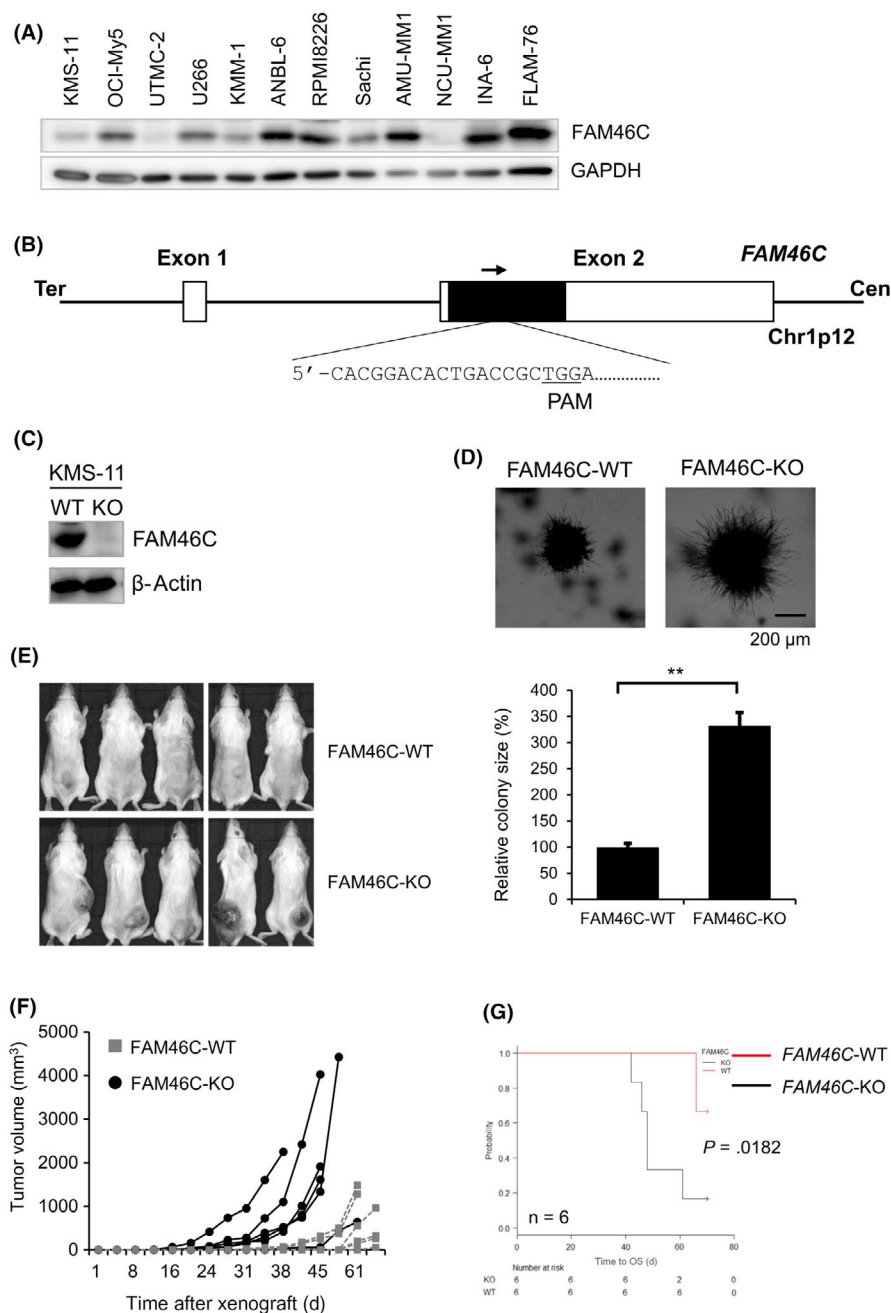
FIGURE 1 Generation of biallelic loss of the *FAM46C* gene in multiple myeloma (MM) cells. A, Western blot analysis showing FAM46C expression in 12 human MM cell lines. Protein lysate (10 μg) was subjected to western blot analysis to detect FAM46C protein. GAPDH was used as an internal control. B, Schematic summary of gene targeting for exon-2 of *FAM46C*. A single guide RNA (arrow) sequence was designed against the exon 2 of *FAM46C* gene loci. C, Western blot analysis of FAM46C protein expression. *FAM46C*-WT and FAM46C-KO cells were seeded in a 6-well plate. D, Cell clones (1000 cells/well) were resuspended in medium containing 0.3% agar and seeded in a 6-well plate (n = 3). Data are expressed relative to the relative colony volume (%) of *FAM46C*-WT KMS-11 cells, which was defined arbitrarily as 100%. The relative colony volume was calculated using the modified ellipsoid formula $1/2$ (length × width^2). ** $P < .005$. E-G, *FAM46C*-WT or *FAM46C*-KO KMS-11 cell clone (2×10^7 cells/mouse) was implanted s.c. in immunodeficient SCID mice. E, Representative photographs of tumor-bearing mice in each group are shown. F, Each line graph shows the tumor volume (mm^3), calculated using the modified ellipsoid formula $1/2$(length × width^2). G, Line graph shows the percentage of mouse survival (n = 6)

the *FAM46Cs* located on chromosome 1p in KMS-11 cells, whereas the copy number of *FAM46C* was intact in ANBL-6 and OCI-My5 cells (Figure S1). In addition, Sanger sequence analysis did not detect *FAM46C* gene mutations in KMS-11, ANBL-6, or OCI-My5 cells (data not shown). To disrupt the *FAM46C* gene in these cell lines, we utilized the CRISPR-Cas9 system by targeting exon-2 of *FAM46C* (Figure 1B). Sequencing analysis confirmed the detection of small indels in the KMS-11 cell lines (Figure S2A). Western blot analysis showed the absence of FAM46C protein in the *FAM46C*-KO cell clones, whereas it was readily detectable in the control *FAM46C*-WT cell clones (Figure 1C), suggesting complete disruption of FAM46C in the *FAM46C*-KO cell clones. We next examined the effect of *FAM46C* disruption on the proliferation of

MM cells. Soft agar-based colony formation assay showed that the size of colonies in *FAM46C*-KO cell clones was significantly larger than that in the *FAM46C*-WT cell clones (Figures 1D and S2B). The MTT assay showed no significant differences in proliferation ratio between the *FAM46C*-KO and *FAM46C*-WT KMS-11 cells (Figure S2C), whereas the *FAM46C*-KO OCI-My5 cells significantly grew faster than the *FAM46C*-WT isogenic control cells (Figure S2D). Based on the in vitro results, we undertook xenograft experiments using immunodeficient SCID mice. Importantly, the tumor growth ratio derived from *FAM46C*-KO cells was substantially faster than that derived from *FAM46C*-WT cells (Figure 1E,F). Furthermore, Kaplan-Meier survival analysis showed significantly shorter survival of xenografted mice with *FAM46C*-KO cell-derived

tumor (*FAM46C*-KO tumor) than with *FAM46C*-WT cell-derived tumor (*FAM46C*-WT tumor) (Figure 1G), suggesting that FAM46C could play a pivotal role in tumorigenesis both in vitro and in vivo.

3.2 | Loss of *FAM46C* upregulates serum-responsible genes and downregulates PTEN-related genes

To delineate the molecular mechanism by which loss of *FAM46C* enhances the proliferation of MM cells, we next undertook comprehensive gene expression analysis and GSEA with OCI-My5, KMS-11, and ANBL-6 cells. Heatmap analysis showed that loss of *FAM46C* showed distinct gene expression profiles from those of *FAM46C*-WT cells (Figure 2A). Notably, GSEA of oncogenic signatures in the *FAM46C*-KO cells indicated significant activation of serum-responsible genes (CSR_EARLY_UP.V1_UP) with significant inactivation of genes related to a tumor suppressor gene, phosphatase and tensin homolog (*PTEN*; PTEN_DN.V1_DN) (Figure 2B,C). Our gene expression analysis also showed that the genes related to PI3K-Akt signaling are upregulated or downregulated in the *FAM46C*-KO MM cells compared to *FAM46C*-WT cells (Tables S3 and S4). Additionally, the GSEA analysis showed significant activation of sonic hedgehog signaling (GCNP_SHH_UP_LATE.V1_UP and GCNP_SHH_UP_EARLY. V1_UP) in the *FAM46C*-KO cells (Figure S3). Furthermore, the result of the GSEA of genes using hallmark gene sets showed significant activation of IL6-JAK-STAT3 related genes in the *FAM46C*-KO cells (HALLMARK_IL6_JAK_STAT3_SIGNALING; Figure 2D). We compared our gene expression data with previously published data (GSE99356 and GSE99358).[16] We found that there were few similarities among the gene expression profiles (Tables S5 and S6).[16] These results suggest that loss of FAM46C enhances cell proliferation by mediating oncogenic gene activation related to serum stimulation or dysregulation of the Akt signaling pathway.

3.3 | Loss of *FAM46C* enhances both in vitro and in vivo phosphorylated Akt levels

As our data suggest that PI3K-Akt signaling could play an important role in the augmented tumorigenesis of *FAM46C*-KO MM cells, we used western blot analysis to investigate the oncogenic molecules associated with the PI3K-Akt signaling pathway. Interestingly, western blot analysis showed increased phosphorylation of Akt at both Thr308 and Ser473 in the *FAM46C*-KO-derived tumors compared to *FAM46C*-WT-derived tumors (Figure 3A). Additionally, we showed an increase in phosphorylated levels of Akt substrates, including FoxO1/3a in the *FAM46C*-KO tumors (Figure 3A). Similar in vitro observations were seen in the clones derived from the KMS-11 and ANBL-6 cells (Figure 3B). We found that the phosphorylation levels of MAPK, including p44/42, slightly but not significantly increased in the *FAM46C*-KO OCI-My5-derived tumors (Figure S4). We examined the effect of exogenous FAM46C expression on phosphorylation levels of Akt and its substrates in the *FAM46C*-KO OCI-My5 cells. We showed that rescuing FAM46C caused decreased Akt and FoxO3a phosphorylation (Figure 3C), but did not change the protein expression of PTEN, which is a negative regulator of PI3K-Akt signaling (Figure 3C). Using a quantitative assay kit, we examined whether *FAM46C* disruption contributes to PTEN activity. Of note, PTEN activity was significantly lower in the *FAM46C*-KO KMS-11 cells than in the *FAM46C*-WT KMS-11 cells (Figure 3D). These results suggest an association between FAM46C expression and the PI3K-Akt signaling pathway.

3.4 | FAM46C disruption increases the cell cycle S-phase ratio

Our protein analysis with the *FAM46C*-KO cells suggests a significant activation of serum stimulation and/or the PI3K-Akt signaling pathway, both of which accelerate the cell cycle and increase cell survival. Therefore, we examined whether FAM46C disruption contributes to cell cycle or apoptosis by FACS analyses using PI and AxV/PI double staining experiments. As expected, the population of S-phase cells increased in all the *FAM46C*-KO MM cells (Figure 4A). In addition, the percentage of apoptotic cells (AxV/PI double-positive cells) decreased slightly in all the *FAM46C*-KO cells (Figure 4B). Furthermore, the caspase-3/7 activity decreased significantly in *FAM46C*-KO cells compared to the *FAM46C*-WT cells (Figure 4C). Similarly, the caspase-8 and caspase-9 activities decreased substantially in the *FAM46C*-KO KMS-11 cells compared to the *FAM46C*-WT cells (Figure 4D). For investigating the role of Akt in caspase activation in MM cells, we examined the effect of constitutively active AKT1 (Myr-AKT1) on caspase activity in the OCI-My5 cells. Caspase-Glo assay showed significantly decreased caspase-8 and caspase-9 activities in cells expressing Myr-AKT1 compared to control cells (Figure 4E). These results suggest that FAM46C might be associated with cell survival by mediating the PI3K-Akt signaling pathway.

3.5 | Sensitivity to anti-MM drugs in *FAM46C*-KO MM cells

The involvement of FAM46C in MM cell sensitivity to anti-MM drugs, LEN, POM, and BOR was examined using the MTT cell viability assay. The MTT assay showed slightly but not significantly reduced cell survival percentage after treatment with LEN in FAM46C-KO KMS-11 cells (Figure 5A), with significantly reduced cell survival percentage after treatment with POM in the *FAM46C*-KO ANBL-6 cells compared to FAM46C-WT cells (Figure 5B). In addition, decreased cell survival percentage was noticed in *FAM46C*-KO ANBL-6 cells but not in KMS-11 cells after treatment with BOR compared to *FAM46C*-WT cells (Figure 5C). To further investigate the involvement of *FAM46C* in the sensitivity of MM cells to anticancer agents, we examined the effect of doxorubicin (DOX) and melphalan (MEL) on MM cell survival. Results of the MTT assay showed significantly increased cell

(A) *FAM46C*

(B)

CSR_EARLY_UP.V1_UP

NES: 1.76
FDR: 4.1%

FAM46C-KO   *FAM46C*-WT

(C)

PTEN_DN_.V1_DN

NES: −1.87
FDR: 1.3%

FAM46C-KO   *FAM46C*-WT

(D)

IL6_JAK_STAT3_SIGNALING

NES: 1.62
FDR: 3.0%

FAM46C-KO   *FAM46C*-WT

FAM46C

FIGURE 2 Gene expression analysis. cDNA microanalysis was carried out using SurePrint G3 Human 8 × 60K V3 format (Agilent). A, Heatmap of the top 50 upregulated and downregulated genes in the *FAM46C*-KO cell clones. The heatmap, with the corresponding gene name on the right side, was constructed using GSEA version 2.2.4 software (Broad Institute). B-D, All raw data were formatted and applied to oncogenic signatures (C6, B-C) or hallmark gene sets (D). Representative GSEA enrichment plots and corresponding heatmap images of the indicated gene sets in *FAM46C*-KO and *FAM46C*-WT cell clones are shown. B, CSR_EARLY_UP.V1_UP signaling. C, KRAS.DF.V1_DN signaling. D, IL6_JAK_STAT3 signaling. Genes contributing to enrichment are shown in rows, and the sample is shown in one column on the heatmap. Expression level is represented as a gradient from high (red) to low (blue). FDR, false discovery rate; NES, normalized enrichment score

survival percentage after treatment with both DOX and MEL in the *FAM46C*-KO KMS-11 and OCI-My5 cells (Figure 5D,E), suggesting that MM cells with *FAM46C* deletion show drug resistance to treatment with DOX and MEL.

3.6 | PI3K-AKT inhibitor, sensitized *FAM46C*-KO MM cells to bortezomib

To delineate the molecular mechanism by which Akt phosphorylation level increased in *FAM46C*-KO MM cells, we examined the effect of specific PI3K-Akt signaling inhibitors, including a potent and selective oral PI3K inhibitor (PF-04691502) and a PDPK1 inhibitor (OSU-03012) on the phosphorylation level of Akt and its substrate FoxO3a in OCI-My5 cells. Intriguingly, western blot analysis showed decreased phosphorylation of Akt at both Thr308 and Ser473 after treatment with PF-04691502, whereas Akt phosphorylation decreased only at Thr308 after treatment with OSU-03012 (Figure 6A). Also, the phosphorylation levels of FoxO3a decreased after treatment with both PF-04691502 and OSU-03012 (Figure 6A). Results of the soft-agar colony formation assay showed that treatment with afuresertib markedly inhibits the colony formation activity of *FAM46C*-KO KMS-11 and OCI-My5 cell clones (Figure 6B). In addition, treatment with PF-04691502 reduced the phosphorylation levels of Akt and FoxO3a in the *FAM46C*-KO KMS-11 cells (Figure S5). These results indicate the likelihood of PI3K involvement in augmenting Akt phosphorylation, induced by *FAM46C* disruption. To examine whether loss of *FAM46C* affects the expression of genes related to PI3K-Akt signaling, we analyzed the expression levels of genes related to PI3K-Akt signaling. We found that the gene expression levels, including *AKT*, *PIK3CA*, *PDPK1*, and *PTEN*, had no significant differences between *FAM46C*-WT and *FAM46C*-KO groups (Figures S6). We also analyzed the correlation between FAM46C expression in MM patients and expression levels of PI3K-Akt signaling molecules using public gene expression data from the HOVON65/GMMG-HD4 cohort study (GSE19784). This analysis showed that there are almost no correlations between gene expression of FAM46C and those of PI3K-Akt signaling (Figures S7), suggesting that loss of function of FAM46C but not its expression level might be related to augmentation of PI3K-Akt signaling in MM. We finally examined the effect of afuresertib, an Akt inhibitor with tumor-specific antiproliferative activity,[32] on the survival of *FAM46C*-KO MM cells. We showed slightly but a significantly lower percentage of cell survival in the *FAM46C*-KO cells after treatment with afuresertib compared to *FAM46C*-WT OCI-My5 cells (Figure 6C). To enhance

the antiproliferative activity induced by anti-MM drugs, we evaluated the effect of afuresertib on bortezomib-induced cytotoxic activity in *FAM46C*-KO MM cells. The MTT assay showed that the combined afuresertib-BOR treatment decreased the survival of the *FAM46C*-KO OCI-My5 cells significantly compared with monotherapy with either drug alone (Figure 6D). Similar results were observed after PI3K inhibitor (PF-04691502) monotherapy or combined PF-04691502-BOR treatment (Figures S8). Collectively, these results suggest that loss of *FAM46C* might enhance cell survival and proliferation by mediating the PI3K-Akt signaling pathway.

4 | DISCUSSION

The present study reports for the first time that loss of *FAM46C*, deleted or mutated in a subset of patients with MM, promotes Akt phosphorylation levels in MM cells both in vitro and in vivo. We also found that both the number of apoptotic cells and caspase-3 activity were higher in the *FAM46C*-KO cell clones than in the *FAM46C*-WT cell clones. Furthermore, mRNA gene expression in the serum-response gene set was significantly upregulated; in contrast, the PTEN-related gene set was significantly downregulated in the *FAM46C*-KO cell clones compared to the *FAM46C*-WT cell clones. Moreover, afuresertib, an ATP-competitive inhibitor, sensitized the *FAM46C*-KO OCI-My5 cells to bortezomib.

The Ser and Thr kinase *AKT*, also known as protein kinase B (PKB), is a well-known oncogene, which augments cell survival and regulates cell death mainly through its kinase activity.[33] The kinase activity of Akt depends on the phosphorylation level at Thr308 and Ser473, both of which are mediated by extracellular growth signaling and subsequent activation of intracellular signaling, including those of PI3K or PDPK1.[33-35] In this study, we showed that *FAM46C* loss increases the phosphorylation levels of Akt at Thr308 and Ser473 both in vitro and in vivo. Consistent with the augmentation of Akt phosphorylation, the phosphorylation of Akt substrate FoxO1/3a, which regulates cell survival and cell proliferation was increased significantly in the FAM46C-KO cells. Furthermore, gene expression profiling showed that loss of *FAM46C* significantly upregulates serum-responsive genes and downregulates the genes related to *PTEN*, which is a well-known negative regulator of PI3K-Akt signaling. In addition to the observations, rescuing FAM46C expression attenuates phosphorylated levels of both Akt and FoxO3a, strongly indicating a close association of FAM46C expression with Akt activity. The phosphorylation levels of PDPK1, (which directly phosphorylates Akt, but does not show PI3K/p110α
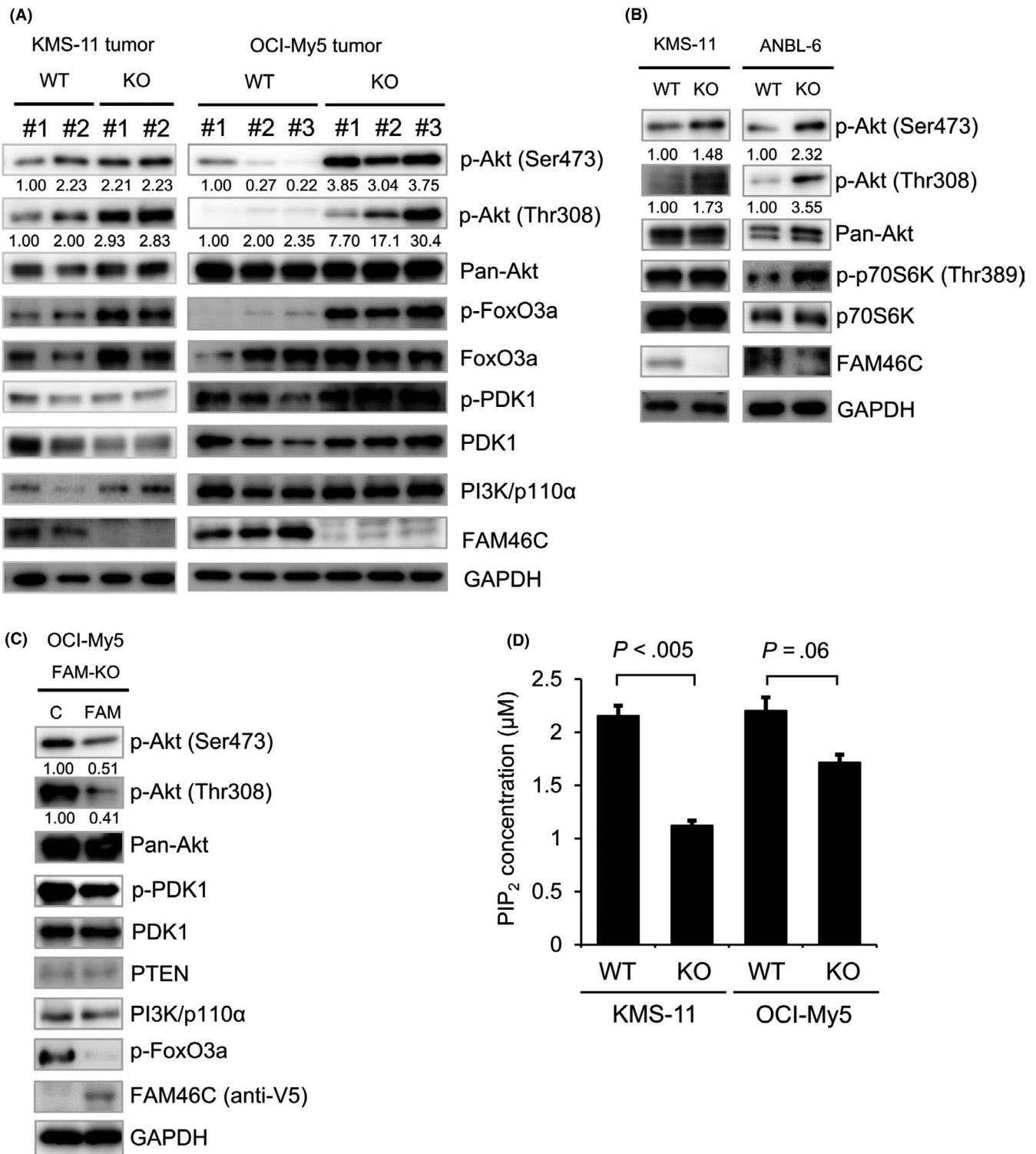
FIGURE 3 Effect of disruption of *FAM46C* on the PI3K-Akt signaling pathway. A-C, Phosphorylation and protein expression levels of molecules involved in PI3K-Akt signaling in vivo (A) and in vitro (B). *FAM46C*-WT and *FAM46C*-KO KMS-11 (left) or OCI-My5 (right) cell-derived tumors from individual xenografted mice were extracted and soluble fractions were subjected to western blot analysis. Values below each blot were expressed as relative phosphorylated Akt (p-Akt) levels, which were calculated after normalization against an internal control, GAPDH. B, Western blot analysis to examine the protein levels of *FAM46C*-WT and *FAM46C*-KO KMS-11 cells (left), and ANBL-6 (right) in vitro. C, Effect of rescuing FAM46C expression on phosphorylation levels of Akt and its substrates. Exogenous FAM46C was tagged with V5 peptide, and its expression detected using anti-V5 tag Ab. D, Effect of disruption of FAM46C on phosphatase and tensin homolog (PTEN) activity. PTEN protein from each cell clone was immunoprecipitated using an anti-PTEN Ab (#9559; Cell Signaling Technology). PTEN activity was measured using a PTEN Activity ELISA kit (Echelon Biosciences). Data are expressed as mean ± SE (n = 3). PIP_2, phosphatidylinositol-4 5-bisphosphate

FIGURE 4 Effect of disruption of *FAM46C* on cell cycle and apoptosis in multiple myeloma cells. A, Cell cycle analysis. Cell clones (2 × 10⁵ cells/well) were seeded in a 12-well plate and were incubated for 48 h. The cell cycle was analyzed with FACSCanto II and FlowJo software. B, Apoptosis assay with annexin V (AxV)-based staining method. Cell clones were seeded and incubated, as described in (A). Bar graphs show the percentage of apoptotic (AxV⁺) cells (n = 3). PI, propidium iodide. C, D, Caspase-3/7, caspase-8, and caspase-9 activities. *FAM46C*-WT and *FAM46C*-KO KMS-11 cell clones were seeded and incubated as described above. E, Effect of constitutively active Myr-Akt1 on caspase activities in OCI-My5 cells. Retroviruses were prepared with either pMSCV-flag-myr-Akt1-IRES-GFP or pMIG II (control) using 293T cells. *P < .05, **P < .005
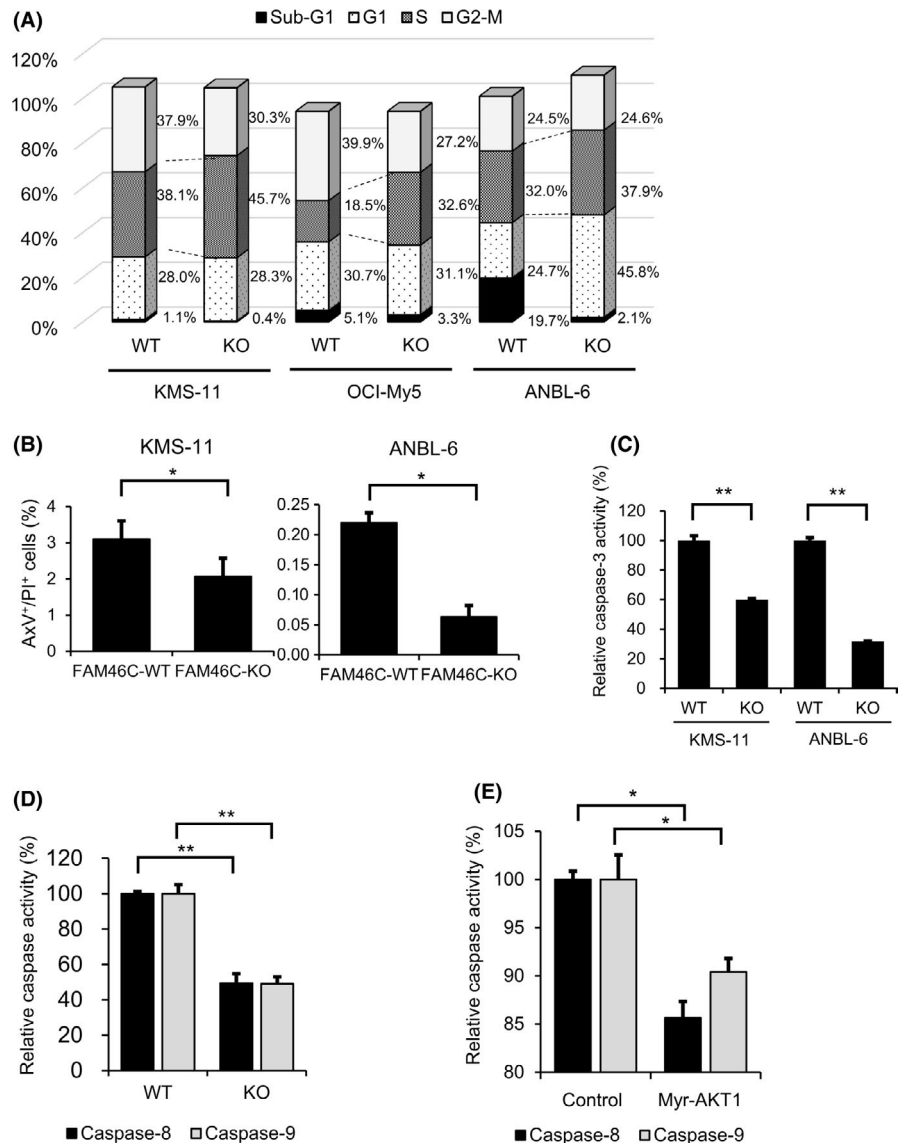
protein expression), increased in the *FAM46C*-KO cells compared to the *FAM46C*-WT cells. In addition, treatment with PI3K inhibitor PF-04691502 and PDPK1 inhibitor OSU-03012 decreased the Akt and FoxO3a phosphorylation levels, suggesting FAM46C could indirectly regulate the phosphorylation levels of Akt. Our microarray analysis also showed that loss of FAM46C does not affect the mRNA expression of genes related to PI3K-Akt signaling. These results suggest that FAM46C might modulate the phosphorylation of Akt by mediating post-transcriptional regulation. Activity of PTEN was observed to be significantly lower in *FAM46C*-KO KMS-11 cells than in *FAM46C*-WT KMS-11 cells, indicating that the increased phosphorylation level of Akt in *FAM46C*-KO MM cells could, at least in part, be mediated by decreased PTEN activity. Protein kinase B activity is reportedly negatively regulated by other phosphatases, including protein phosphatase 2A, inositol polyphosphate-4-phosphatase type II, and PH domain leucine-rich repeat protein phosphatase-1, and positively regulated by mTORC2.[33,36-38] As our data do not necessarily clarify the molecular function of FAM46C on PI3K-Akt signaling, further studies are warranted to uncover the

molecular mechanism by which loss of FAM46C promotes PI3K-Akt signaling in MM cells.

It has been reported that PI3K-Akt pathway plays an important role in the pathogenesis of MM.[39] Activation of PI3K-Akt signaling confers tumor progression to MM cells.[15] Therefore, targeting the PI3K-Akt pathway using current standard chemotherapeutics is a novel therapeutic strategy to improve the clinical outcome of patients with MM.[40-45] In this study, we also showed that an ATP-competitive Akt inhibitor, afuresertib, as well as an ATP-competitive PI3K/mTOR dual inhibitor, PF-04691502, enhances the cytotoxicity induced by BOR or immunomodulatory drugs. As phosphorylation levels of Akt were augmented significantly in the *FAM46C*-KO cells compared to those in *FAM46C*-WT cells, Akt targeting could be beneficial for MM patients with LOH or mutation of the *FAM46C* gene.

Association of LOH or mutation of *FAM46C* with impaired survival of patients with MM was shown earlier.[13] Mroczek et al have reported that *FAM46C*, also called *TENT5C*, acts as a tumor suppressor in MM cells.[19] They showed that FAM46C increases the polyadenylation of selected mRNAs, including signal-sequence receptor
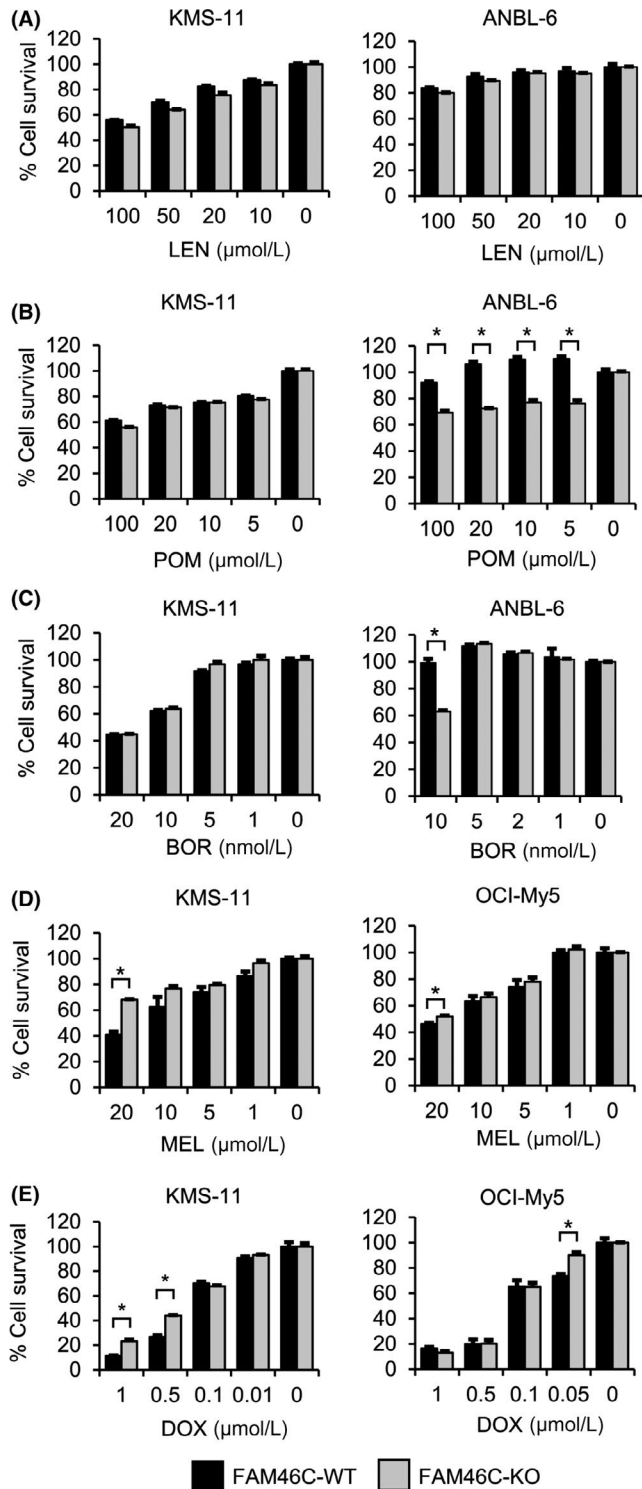
FIGURE 5 Effect of antimyeloma drugs on the survival of *FAM46C*-KO cell clones. A-C, MTT assay was undertaken with *FAM46C*-KO and *FAM46C*-WT cell clones. Cells were treated with the indicated concentration of antimyeloma drugs for 72 h: (A) lenalidomide (LEN; 100, 20, 10, 5, or 0 μM), (B) pomalidomide (POM; 100, 20, 10, 5, or 0 μM), (C) bortezomib (BOR; KMS-11, 20, 10, 5, 1, or 0 nM; ANBL-6, 10, 5, 2, 1, or 0 nM), (D) melphalan (MEL; KMS-11 and OCI-My5, 20, 10, 5, 1, or 0 μM), and (E) doxorubicin (DOX; KMS-11, 1.0, 0.5, 0.1, 0.05, or 0 μM; OCI-My5, 1.0, 0.5, 0.1, 0.01, or 0 μM). Data are expressed relative to the mean optic density (595 nm) of untreated cells, which was defined arbitrarily as 100%. Data are expressed as mean ± SE (n = 3). *P < .05

effect of FAM46C and its mutants on Akt phosphorylation level and changes in gene expression.

Recently, Zhu et al[16] have reported that loss of FAM46C confers relative resistance to dexamethasone and LEN treatments. In this study, we showed varying sensitivities to anti-MM drugs among the MM cell lines, with lower sensitivities to anticancer agents (DOX and MEL) in *FAM46C*-KO MM cells compared with *FAM46C*-WT cells. Resistance of *FAM46C*-KO MM cells toward DOX and MEL might be due to increased caspase activities. Contrarily, *FAM46C*-KO ANBL-6 cells sensitized to treatment with POM and BOR. Indeed, the survival of ANBL-6 cells completely depends upon presence of IL-6, which activates various signaling pathways including Akt. As POM and BOR are known to inhibit the phosphorylation of Akt, it might be possible that loss of *FAM46C* increases the dependency of the survival of MM cells on PI3K-Akt signaling in ANBL-6 cells. These results suggest that POM and BOR might be effective for some patients with *FAM46C* deletion (Figure 5B,C). Given the fact that each cell line has different genomic alterations, it might be possible that anti-MM drugs are influenced by additional cooccurring genetic alterations in MM cells with biallelic loss of the *FAM46C* gene. Additional studies are warranted to understand the association between drug susceptibilities and patients with MM harboring the *FAM46C* gene abnormality.

In conclusion, this the first study to show that loss of FAM46C enhances phosphorylation levels of Akt both in vitro and in vivo. Our results raise the possibility that the enhanced phosphorylation of Akt and its substrate could be linked to a refractory phenotype of MM cells, caused by the disruption of the *FAM46C* gene. Although we showed an additive antiproliferative effect of PI3K-Akt inhibitors in FAM46C-KO cells only in vitro, it is possible that combined treatment with anti-MM drugs and PI3K-Akt inhibition might coordinately suppress the tumor growth of MM cells with any LOH or mutation of *FAM46C*. Thus, an understanding of molecular characteristics of refractory/relapsed MM could be utilized to develop a targeted genomic therapy and novel molecular-targeted strategies, which could lead to improved clinical outcomes in patients with MM.

subunit delta 4 (*SSR4*) in MM cells. In this study, the gene expression profiling showed a decrease in mRNA expression of *SSR4* in the FAM46C-KO MM cells, suggesting that FAM46C might enhance the stability of *SSR4* mRNA in MM cells. As polyadenylation of RNA promotes not only nuclear export of RNA, translation initiation, and transcript stability but also RNA degradation,[46,47] polyadenylation activity of FAM46C might affect the function and expression of selected mRNAs. Therefore, it would be of interest to examine the
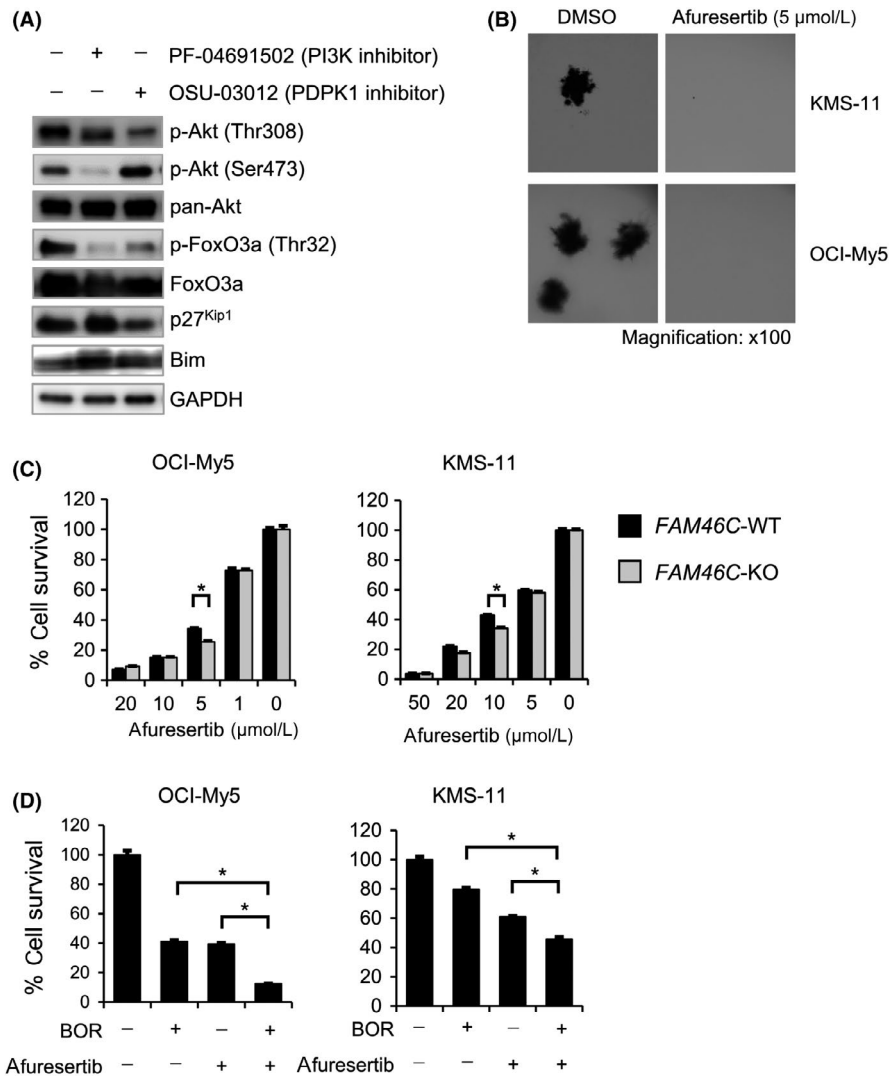
FIGURE 6 Effect of specific AKT inhibitor, afuresertib, and its combination with bortezomib on the survival of *FAM46C*-KO cell clones. A, Effect of specific PI3K-Akt signaling inhibitors on phosphorylation level of Akt and its substrate, FoxO3a, in *FAM46C*-KO multiple myeloma cells. *FAM46C*-KO KMS-11 cells were treated with either PF-04691502 (a PI3K inhibitor, 0.1 μM) or OSU-03012 (3-phosphoinositide dependent protein kinase 1 [PDPK1] inhibitor, 10 μM) for 16 h. Cells were lysed in loading buffer, and the cell lysates were subjected to western blot analysis. B, Effect of afuresertib on the colony formation activity of *FAM46C*-KO KMS-11 and OCI-My5 cells. Cells were treated with afuresertib (5 μM). Photographs depicting the results of the colony formation assay are shown. C, Effect of afuresertib on the survival of *FAM46C*-WT (black bar) and *FAM46C*-KO (gray bar) KMS-11 cells. KMS-11 cells were seeded and treated with the indicated concentration (OCI-My5, 20, 10, 5, 1, or 0 μM; KMS-11, 50, 20, 10, 5, or 0 μM) of afuresertib for 72 h. Percentage survival of the cell clones was measured by MTT assay. D, Effect of combined treatment of afuresertib with bortezomib on the survival of *FAM46C*-KO OCI-My5 (left) or KMS-11 (right) cells. Cells were treated with the indicated concentration of afuresertib (5 μM) and bortezomib (BOR; 10 nM) for 72 h. Data are expressed as mean ± SE (n = 3). *$P < .05$ (n = 3)

DISCLOSURE

ETHICAL APPROVAL

This research complies with the ethical guidelines of the Japanese Ministry of Health, Labour, and Welfare.

ORCID

Ichiro Hanamura https://orcid.org/0000-0002-6681-8927
Akinobu Ota https://orcid.org/0000-0002-6296-2921
Sivasundaram Karnan https://orcid.org/0000-0003-2165-7565

REFERENCES

1. Kumar SK, Rajkumar V, Kyle RA, et al. Multiple myeloma. *Nat Rev Dis Primers*. 2017;3:17046.
2. Anderson KC, Alsina M, Bensinger W, et al. Multiple myeloma. *J Natl Compr Canc Netw*. 2011;9(10):1146-1183.
3. Moreau P, San Miguel J, Sonneveld P, et al. Multiple myeloma: ESMO Clinical Practice Guidelines for diagnosis, treatment and follow-up. *Ann Oncol*. 2017;28(suppl_4):;iv52-iv61.
4. Gandolfi S, Vekstein C, Laubach JP, et al. The evolving role of transplantation in multiple myeloma: the need for a heterogeneous approach to a heterogeneous disease. *Clin Adv Hematol Oncol*. 2018;16(8):564-574.
5. Hoang PH, Dobbins SE, Cornish AJ, et al. Whole-genome sequencing of multiple myeloma reveals oncogenic pathways are targeted somatically through multiple mechanisms. *Leukemia*. 2018;32(11):2459-2470.
6. Robiou du Pont S, Cleynen A, Fontan C, et al. Genomics of multiple myeloma. *J Clin Oncol*. 2017;35:963-967.
7. Walker BA, Boyle EM, Wardell CP, et al. Mutational spectrum, copy number changes, and outcome: results of a sequencing study of patients with newly diagnosed myeloma. *J Clin Oncol*. 2015;33:3911-3920.
8. Lohr JG, Stojanov P, Carter SL, et al. Widespread genetic heterogeneity in multiple myeloma: implications for targeted therapy. *Cancer Cell*. 2014;25:91-101.
9. Bolli N, Avet-Loiseau H, Wedge DC, et al. Heterogeneity of genomic evolution and mutational profiles in multiple myeloma. *Nat Commun*. 2014;5:2997.
10. Manier S, Salem KZ, Park J, Landau DA, Getz G, Ghobrial IM. Genomic complexity of multiple myeloma and its clinical implications. *Nat Rev Clin Oncol*. 2017;14:100-113.
11. Boyd KD, Ross FM, Walker BA, et al. Mapping of chromosome 1p deletions in myeloma identifies FAM46C at 1p12 and CDKN2C at 1p32.3 as being genes in regions associated with adverse survival. *Clin Cancer Res*. 2011;17(24):7776-7784.
12. Chapman MA, Lawrence MS, Keats JJ, et al. Initial genome sequencing and analysis of multiple myeloma. *Nature*. 2011;471(7339):467-472.
13. Walker BA, Mavrommatis K, Wardell CP, et al. Identification of novel mutational drivers reveals oncogene dependencies in multiple myeloma. *Blood*. 2018;132(6):587-597.
14. Barbieri M, Manzoni M, Fabris S, et al. Compendium of FAM46C gene mutations in plasma cell dyscrasias. *Br J Haematol*. 2016;174:642-645.
15. Younes H, Leleu X, Hatjiharissi E, et al. Targeting the phosphatidylinositol 3-kinase pathway in multiple myeloma. *Clin Cancer Res*. 2007;13:3771-3775.
16. Zhu YX, Shi CX, Bruins LA, et al. Loss of FAM46C promotes cell survival in myeloma. *Cancer Res*. 2017;77:4317-4327.
17. Mroczek S, Chlebowska J, Kuliński TM, et al. The non-canonical poly(A) polymerase FAM46C acts as an onco-suppressor in multiple myeloma. *Nat Commun*. 2017;8:619.
18. Kharas MG, Okabe R, Ganis JJ, et al. Constitutively active AKT depletes hematopoietic stem cells and induces leukemia in mice. *Blood*. 2010;115:1406-1415.
19. Holst J, Szymczak-Workman AL, Vignali KM, Burton AR, Workman CJ, Vignali DA. Generation of T-cell receptor retrogenic mice. *Nat Protoc*. 2006;1:406-417.
20. Ozaki S, Wolfenbarger D, deBram-Hart M, Kanangat S, Weiss DT, Solomon A. Characterization of a novel interleukin-6 autocrine-dependent human plasma cell line. *Leukemia*. 1994;8:2207-2213.
21. Jelinek DF, Ahmann GJ, Greipp PR, et al. Coexistence of aneuploid subclones within a myeloma cell line that exhibits clonal immunoglobulin gene rearrangement: clinical implications. *Cancer Res*. 1993;53:5320-5327.
22. Takahashi M, Ota A, Karnan S, et al. Arsenic trioxide prevents nitric oxide production in lipopolysaccharide -stimulated RAW 264.7 by inhibiting a TRIF-dependent pathway. *Cancer Sci*. 2013;104:165-170.
23. Wahiduzzaman M, Ota A, Karnan S, et al. Novel combined Ato-C treatment synergistically suppresses proliferation of Bcr-Abl-positive leukemic cells in vitro and in vivo. *Cancer Lett*. 2018;433:117-130.
24. Ran FA, Hsu PD, Wright J, Agarwala V, Scott DA, Zhang F. Genome engineering using the CRISPR-Cas9 system. *Nat Protoc*. 2013;8:2281-2308.
25. Sanjana NE, Shalem O, Zhang F. Improved vectors and genome-wide libraries for CRISPR screening. *Nat Methods*. 2014;11:783-784.
26. Stewart SA, Dykxhoorn DM, Palliser D, et al. Lentivirus-delivered stable gene silencing by RNAi in primary cells. *RNA*. 2003;9:493-501.
27. Ota A, Nakao H, Sawada Y, et al. Δ40p53α suppresses tumor cell proliferation and induces cellular senescence in hepatocellular carcinoma cells. *J Cell Sci*. 2017;130:614-625.
28. Hossain E, Ota A, Karnan S, et al. Lipopolysaccharide augments the uptake of oxidized LDL by up-regulating lectin-like oxidized LDL receptor-1 in macrophages. *Mol Cell Biochem*. 2015;400:29-40.
29. Subramanian A, Tamayo P, Mootha VK, et al. Gene set enrichment analysis: a knowledge-based approach for interpreting genome-wide expression profiles. *Proc Natl Acad Sci USA*. 2005;102:15545-15550.
30. Mootha VK, Lindgren CM, Eriksson KF, et al. PGC-1alpha-responsive genes involved in oxidative phosphorylation are coordinately downregulated in human diabetes. *Nat Genet*. 2003;34:267-273.
31. Kanda Y. Investigation of the freely available easy-to-use software 'EZR' for medical statistics. *Bone Marrow Transplant*. 2013;48:452-458.
32. Yamaji M, Ota A, Wahiduzzaman M, et al. Novel ATP-competitive Akt inhibitor afuresertib suppresses the proliferation of malignant pleural mesothelioma cells. *Cancer Med*. 2017;6:2646-2659.
33. Manning BD, Toker A. AKT/PKB signaling: navigating the network. *Cell*. 2017;169:381-405.
34. Mayer IA, Arteaga CL. The PI3K/AKT pathway as a target for cancer treatment. *Annu Rev Med*. 2016;67:11-28.
35. Hemmings BA, Restuccia DF. The PI3K-PKB/Akt pathway. *Cold Spring Harb Perspect Biol*. 2015;7:pii: a026609.
36. Li CC, Lunardi A, Gulluni F, et al. In vivo role of INPP4B in tumor and metastasis suppression through regulation of PI3K-AKT signaling at endosomes. *Cancer Discov*. 2015;5:740-751.
37. Gao T, Furnari F, Newton AC. PHLPP: a phosphatase that directly dephosphorylates Akt, promotes apoptosis, and suppresses tumor growth. *Mol Cell*. 2005;18:13-24.
38. Sarbassov DD, Guertin DA, Ali SM, Sabatini DM. Phosphorylation and regulation of Akt/PKB by the rictor-mTOR complex. *Science*. 2005;307:1098-1101.
39. Mimura N, Hideshima T, Shimomura T, et al. Selective and potent Akt inhibition triggers anti-myeloma activities and enhances fatal endoplasmic reticulum stress induced by proteasome inhibition. *Cancer Res*. 2014;74:4458-4469.
40. Hideshima T, Catley L, Yasui H, et al. Perifosine, an oral bioactive novel alkylphospholipid, inhibits Akt and induces in vitro

and in vivo cytotoxicity in human multiple myeloma cells. *Blood.* 2006;107:4053-4062.

41. Ikeda H, Hideshima T, Fulciniti M, et al. PI3K/p110{delta} is a novel therapeutic target in multiple myeloma. *Blood.* 2010;116:1460-1468.

42. Kinoshita S, Ri M, Kanamori T, et al. Potent antitumor effect of combination therapy with sub-optimal doses of Akt inhibitors and pomalidomide plus dexamethasone in multiple myeloma. *Oncol Lett.* 2018;15:9450-9456.

43. Jakubowiak AJ, Richardson PG, Zimmerman T, et al. Perifosine plus lenalidomide and dexamethasone in relapsedand relapsed/refractory multiple myeloma: a Phase I Multiple Myeloma Research Consortium study. *Br J Haematol.* 2012;158:472-480.

44. Richardson PG, Wolf J, Jakubowiak A, et al. Perifosine plus bortezomib and dexamethasone in patients with relapsed/refractory multiple myeloma previously treated with bortezomib: results of a multicenter phase I/II trial. *J Clin Oncol.* 2011;29:4243-4249.

45. Ruggero D, Sonenberg N. The Akt of translational control. *Oncogene.* 2005;24:7426-7434.

46. Slomovic S, Fremder E, Staals RH, Pruijn GJ, Schuster G. Addition of poly(A) and poly(A)-rich tails during RNA degradation in the cytoplasm of human cells. *Proc Natl Acad Sci USA*. 2010;107:7407-7412.

47. Slomovic S, Laufer D, Geiger D, Schuster G. Polyadenylation of ribosomal RNA in human cells. *Nucleic Acids Res.* 2006;34:2966-2975.

SUPPORTING INFORMATION

Additional supporting information may be found online in the Supporting Information section.